*Experimental results:* Based on the design in Fig. 1, a network was constructed. A functional test on the network was carried out to check its CM/DM discrimination capability. In the frequency range 10kHz–50MHz, the lowest CM and DM rejection ratios were found to be 38 and 33dB, respectively. Hence, the network is able to isolate the CM or DM signal sufficiently for EMI diagnosis purposes. To demonstrate its practical application, a 24W switched-mode power supply (ASTEC model: RBS22) with 100% loading was used as an EUT. With all the power line EMI filter components in the EUT removed, the conducted emissions of the live and neutral wires measured by the LISN are given in Fig. 2. It is obvious that the EUT failed to comply with EN 55022 class B limits [4] but the measurement does provide some useful clues for EMI diagnosis purposes. Connecting the discrimination network to the LISN, the CM and DM conducted emissions were measured separately.
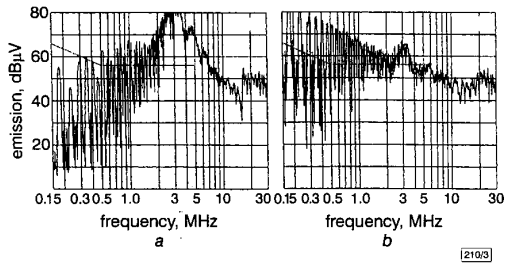

Fig. 3 *CM and DM emissions without filter*

a CM
b DM

Fig. 3 shows clearly that the CM emissions dominate in the 1.5 to 8MHz range, whereas the DM emissions dominate at the lower frequency end of 150kHz to 1MHz. Since the dominant conduction mode at a specific frequency range is identified, appropriate CM or DM EMI filter components will be added accordingly. As a start, a 5mH CM choke was inserted into the power line input of the EUT, and the CM and DM emissions were measured again.
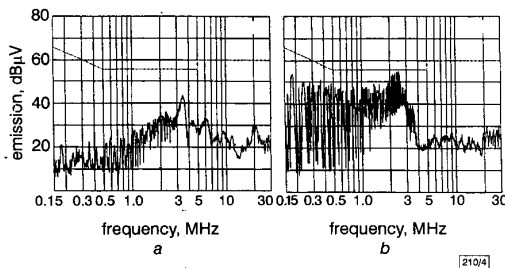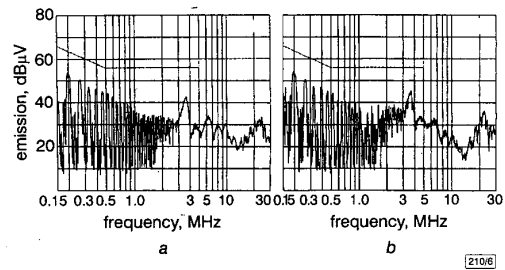

Fig. 4 *CM and DM emissions with CM choke*

a CM
b DM
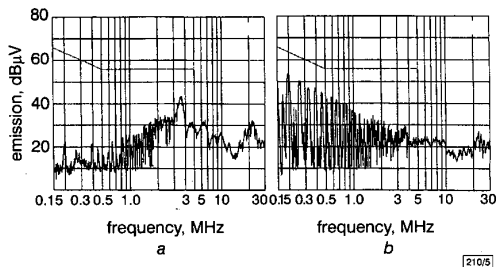
Fig. 5 *CM and DM emissions with CM choke and DM capacitor*

a CM
b DM

Fig. 4 shows that the CM emissions are suppressed significantly below the limits. The leakage inductance of the CM choke also serves as a DM inductance, which attenuates the DM emissions but not as much as those of the CM emissions. To provide com-

fortable EMI margins for the DM emissions at ~2MHz, a 0.1µF capacitor was added across the live and neutral lines of the EUT. Fig. 5 shows that the capacitor has no impact on the CM emissions but it reduces the DM emissions further. Both the CM and DM emissions are now well below the limits. As a final check for EMI compliance, the discrimination network was removed from the LISN, and the conducted emissions for the live and neutral line were measured again. Fig. 6 shows that the EUT has now complied with the limits.

Fig. 6 *Live and neutral emissions with CM choke and DM capacitor*

a Live
b Neutral

Conclusion: A novel CM/DM discrimination network has been developed and has proven to be a useful tool for conducted EMI diagnosis.

Acknowledgment: The author would like to thank his student, K.W. Ow-Yeong, for the construction of the network.

References

1 NAVE, M.J.: 'Power line filter design for switched-mode power supplies' (Van Nostrand Reinhold, USA, 1991)
2 PAUL, C.R., and HARDIN, K.B.: 'Diagnosis and reduction of conducted noise emissions', *IEEE Trans. Electromagn. Compat.*, 1988, **30**, (4) pp. 553–560
3 SMITH, J.: 'Modern communication circuits' (McGraw Hill, USA, 1986)
4 EN 55022: 'Limits and methods of measurement of radio disturbance characteristics of information technology equipment' (British Standards Institution, 1998)

Worst-month rain statistics for radiowave propagation study in Malaysia

J. Chebil and T. Abd. Rahman

A study of the worst-month rainfall rate statistics for the Malaysian environment is presented. Rain rate data with 1 min integration time were collected in the Universiti Teknologi Malaysia and the Universiti Sains Malaysia. The relationship between the worst month and the yearly probabilities is presented and the ITU-R model verified. For better precision, new values are proposed for the parameters Q_1 and β in Malaysia.

Introduction: Rainfall is a serious cause of attenuation for radiowave propagation at frequency bands above 10GHz. It is important to accurately predict the fading outage due to rain attenuation. Although the prediction method recommended by the ITU-R is suitable for temperate regions, it is not as suitable for tropical and equatorial regions. This is due mainly to the lack of rainfall and rain attenuation data in these regions. Rain attenua-

tion studies have been conducted in the Universiti Teknologi Malaysia (UTM) and Universiti Sains Malaysia (USM). Rain data were collected in four locations: Kuala Lumpur, Skudai, Sri Iskandar and Bota. In this Letter, we present a study of the worst-month statistics, which is of importance to the designers of tele-communication systems. The collected data are used to derive the annual worst-month statistics and its relationship with the average annual distribution. This relationship was found to be close to that anticipated by the ITU-R.

Definition of worst-month: The ITU-R [1] has recommended a definition for worst-month statistics, which can be applied to quantities such as rain rate and rain attenuation. For a period of 12 consecutive calendar months, the annual worst month for a preselected threshold is defined as the month (or 30 day period) with the highest probability of exceeding that threshold. A worst month can therefore be established for each threshold level. For ease of description [2], let X_{ij} be the probability of exceeding a threshold level j in the ith month. The worst month for level j is the month with the highest X_{ij} value, X_{hj}. The calendar month to which X_{hj} belongs may vary from one threshold to another. The worst-month distribution for a particular year is given by X_{hj} as a function of j and is the envelope of the highest monthly probability value of all the monthly cumulative distributions from that year. For multiple year data, the average annual worst-month probability is formed by taking averages of the individual annual worst-month probabilities for each level j.

Conversion of annual statistics to worst-month statistics: Worst-month statistics are related to annual statistics by the parameter Q, which is the ratio between the worst-month and annual probability and is given by

$$Q = X/Y \qquad (1)$$

where X is the average worst-month probability and Y is the average annual probability. For simplicity, the i and j subscripts have been eliminated. An extensive study of the relationship between worst-month and annual statistics was conducted by the ITU-R [3]. They determined that Q and Y could be approximated by a power law relationship of the form

$$Q = Q_1 Y^{-\beta} \quad \text{for} \quad (Q_1/12)^{1/\beta}\% < Y < 3\% \qquad (2)$$

where Q_1 and β are two parameters. To relate X to Y, eqn. 2 has been rewritten as

$$X = Q_1 Y^{(1-\beta)} \qquad (3)$$

The ITU-R states that values of $Q_1 = 2.85$ and $\beta = 0.13$ can be used for global planning purposes. They also recommend the values $Q_1 = 1.7$ and $\beta = 0.22$ for Indonesia which is a tropical region close to Malaysia. In our analysis, the latter values will be used.

Experimental results and analysis: Rainfall data with an integration time of 1 min were collected at four locations in Malaysia: UTM-Kuala Lumpur campus (UTM-KL), UTM-Skudai campus (UTM-Skudai), Sri Iskandar and Bota. For UTM-KL (3°08'N, 101°39'E), the data were collected from January 1992 until May 1995 with 94.9% availability. The rain rate was measured by a fast response OSK rain gauge of tipping-bucket type with sensitivity 0.5mm. In UTM-Skudai (1°33'N, 103°38'E), the data were collected from February 21, 1996 until February 20, 1997 with 100% availability. The rain gauge used was of Casella type with a sensitivity of 0.5mm per tip. Similar rain rate measurements were obtained for two years, from July 1992 to June 1994, both in the USM-Sri Iskandar campus and in Sekolah Menangah Vokesional-Bota. The rain gauges used were also of Casella type. The availability of each set of 1 min rain rate data is greater than 92%. The two sites, in Sri Iskandar and Bota, are 3 km apart and the average results obtained from their data can adequately represent the rainfall characteristics in the USM campus (4°22'N, 101°E).

From the measured data, the average 1 min rain rate cumulative distributions were determined at UTM-KL, UTM-Skudai and USM. These distributions were used in eqn. 3 to determine the ITU-R prediction for the worst-month statistics at these locations. The results are compared with the results for the measured aver-

age worst month in Figs. 1 - 3, which show that the ITU-R approximation is in good agreement with the data.
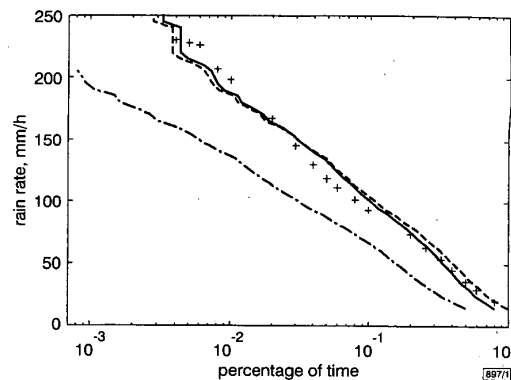

Fig. 1 *Measured worst-month and yearly distribution in UTM-KL, and ITU-R prediction and best-fit model*

+ + + measured
− − − − ITU-R
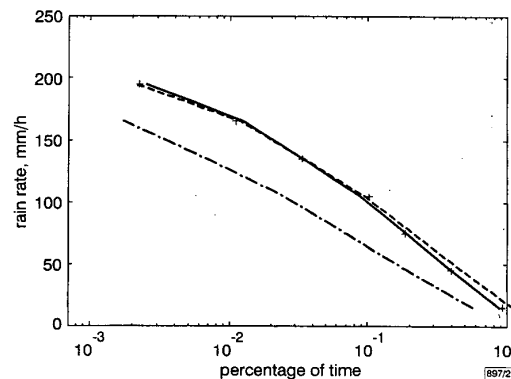———— best fit
— · — yearly

Fig. 2 *Measured worst-month and yearly distribution in UTM-Skudai and ITU-R prediction and best-fit model*

+ + + measured
− − − − ITU-R
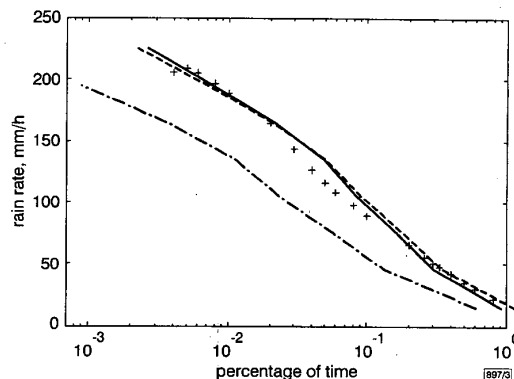———— best fit
— · — yearly

Fig. 3 *Measured worst-month and yearly distribution in USM, and ITU-R prediction and best-fit model*

+ + + measured
− − − − ITU-R
———— best fit
— · — yearly

Table 1 shows the values for the regression parameters Q_1 and β which are determined from the measured data using the least squares method. The values of these parameters at UTM-KL, UTM-Skudai and USM are close and their average can represent both locations. Figs. 1 - 3 show that the fitted curves are generally closer to the measured worst-month distribution than those of

the ITU-R model. Therefore, we suggest that the worst-month relation in eqn. 3 with the recommended values $Q_1 = 1.32$ and $\beta = 0.27$ can be used in the Malaysian environment.

Table 1: Measured values for Q_1 and β in Malaysia

	Q_1	β
UTM-KL	1.22	0.28
UTM-Skudai	1.42	0.25
USM-SMV	1.37	0.26
Average	1.32	0.27

Conclusion: The worst-month statistics on rainfall rate are very useful in designing high quality communication networks since the maximum occurrence of events that lead to the degradation of the network is expected to be higher in the worst month. It is experimentally verified that the power law relation in eqn. 3 with the ITU-R recommended values for Q_1 and β can safely be used for estimating the worst-month statistics in Malaysia. New values for the parameters Q_1 and β are proposed in order to obtain a better estimate for the worst-month statistics in Malaysia.

Acknowledgments: The authors wish to thank the University of Technology Malaysia and Cellular Communication Network (M) Sdn. Bhd. for supporting the research. They also thank S.I.S. Hassen and Lee Leong Hoong for providing the USM data.

References

1 ITU-R Recommendations 1994, PN. 581–2: 'The concept of worst-month', p. 248
2 CRANE, R.K., and DEBRUNNER, W.E.: 'Worst-month statistics', *Electron. Lett.*, 1978, **14**, (2), pp. 38–40
3 ITU-R Recommendations 1994, PN. 841: 'Conversion of annual statistics to worst-month statistics', pp. 249–251

Accurate analytical model for MPEG coded video traffic

H. Liu, N. Ansari and Y.Q. Shi

Self-similar processes, modulated according to the MPEG GOP (group of pictures) structure, are proposed to accurately capture both the SRD (short range dependency) and LRD (long range dependency) of MPEG video traffic.

Introduction: Traffic generated by video applications is increasingly cramming existing networks, and it is thus essential to accurately characterise video traffic for efficient network management. Traditional models, however, fall short in describing video traffic which is strongly autocorrelated and bursty [1]. Hence, autocorrelations among data should be taken into consideration.

The empirical data used here was MPEG coded data for the film Star Wars [Note 1]. The frames were organised as follows: IBBPBBPBBPBB IBBPBB..., i.e. 12 frames in a group of pictures (GOP). I, P, and B frames were compressed by different techniques. It is clear that the autocorrelation function (ACF) of the MPEG coded video, shown in Fig. 1, can hardly be captured by a simple random process.

Modelling MPEG coded data: The MPEG coded data are first decomposed into 10 subsequences X_I, X_P, X_{B1}, X_{B2}, ..., and X_{B8}.

Note 1: The MPEG coded data were courtesy of M.W. Garrett of Bellcore and M. Vetterli of UC Berkeley.

X_I consists of all I frames, X_P all P frames, X_{B1} the first B frames in all GOPs, X_{B2} the second B frames in all GOPs, and so on. We have used $k^{-\beta}$, $e^{-\beta k}$ and $e^{-\beta\sqrt{k}}$ (k is the lag between frames, and β is a constant), corresponding to the ACFs of a self-similar process [2], a Markov process, and an $M/G/\infty$ input process [3], respectively, to approximate the ACFs of these subsequences. Self-similar processes were found to provide the best approximations. For illustrative purposes, approximations for P and B_1 are shown in Figs. 2 and 3, respectively.
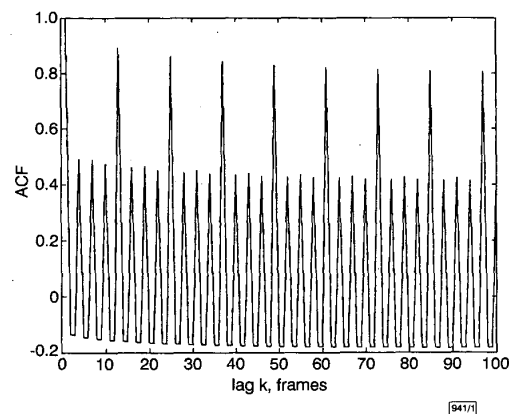

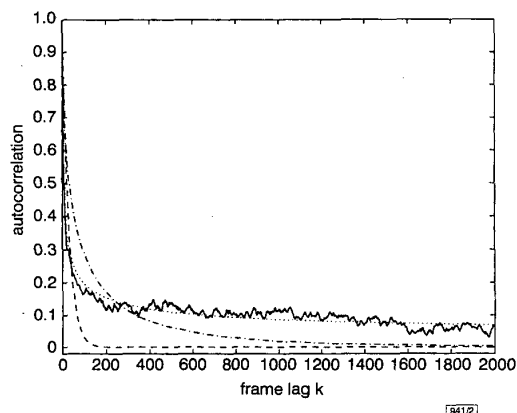
Fig. 1 *ACF of MPEG compressed video of Star Wars*

Fig. 2 *Approximation for ACF of P frames*

.... self-similar process
———— empirical trace
· — · — · M/G/infinity
— — — — Markov process

Using the least squares method, $\beta = 0.4663$, 0.3546, 0.4468, 0.4779, 0.4294, 0.4656, 0.4380, 0.4682, 0.4465, and 0.4606 are obtained for X_I, X_P, X_{B1}, X_{B2}, ..., and X_{B8}, respectively. The corresponding Hurst parameters ($H = 1-\beta/2$) for these processes are $H = 0.7668$, 0.8227, 0.7766, 0.7610, 0.7853, 0.7672, 0.7810, 0.7659, 0.7768, and 0.7697, respectively.

Marginal distributions of these subsequences are modelled by Beta distributions which have the following form of probability density function:

$$f(x; \gamma, \eta, \mu_0, \mu_1) =$$
$$\begin{cases} \frac{1}{\mu_1-\mu_0} \frac{\Gamma(\gamma+\eta)}{\Gamma(\gamma)\Gamma(\eta)} \left(\frac{x-\mu_0}{\mu_1-\mu_0}\right)^{\gamma-1} \left(1 - \frac{x-\mu_0}{\mu_1-\mu_0}\right)^{\eta-1} \\ \qquad\qquad\qquad \mu_0 \leq x \leq \mu_1, 0 < \gamma, 0 < \eta \\ 0 \qquad\qquad\qquad\qquad\qquad \text{otherwise} \end{cases} \quad (1)$$

where γ and η are the shape parameters, and $[\mu_0, \mu_1]$ is the domain where the distribution is defined. Using the formulas introduced in [4], the estimated shape parameters $\eta = 1.5237$, 1.5699, 1.4172, 1.3016, 1.6858, 1.6329, 1.7276, 1.4218, 4.0585, 1.5402, and $\gamma = 12.7263$, 11.1939, 8.1089, 8.1604, 11.8499, 13.9278, 12.2180, 8.6536, 10.4233, 11.1768 are obtained for X_I, X_P, X_{B1}, X_{B2}, ..., and X_{B8}, respectively.